

RSC Advances



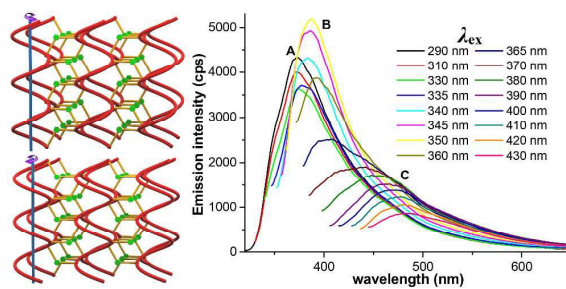
This is an *Accepted Manuscript*, which has been through the Royal Society of Chemistry peer review process and has been accepted for publication.

Accepted Manuscripts are published online shortly after acceptance, before technical editing, formatting and proof reading. Using this free service, authors can make their results available to the community, in citable form, before we publish the edited article. This *Accepted Manuscript* will be replaced by the edited, formatted and paginated article as soon as this is available.

You can find more information about *Accepted Manuscripts* in the [Information for Authors](#).

Please note that technical editing may introduce minor changes to the text and/or graphics, which may alter content. The journal's standard [Terms & Conditions](#) and the [Ethical guidelines](#) still apply. In no event shall the Royal Society of Chemistry be held responsible for any errors or omissions in this *Accepted Manuscript* or any consequences arising from the use of any information it contains.

Graphical Abstract



A solvothermally synthesized 3-D Cd(II) metal-organic framework with rutile topology was found containing right- or left- handed helices in its structure, and emitting tunable UV-to-visible photoluminescence.



Journal Name

COMMUNICATION

A 3-D Metal-Organic Framework with Rutile Topology Network, Right- or Left- Handed Helical Chains and Tunable UV-to-visible Photoluminescence†

Received 00th January 20xx,
Accepted 00th January 20xx

DOI: 10.1039/x0xx00000x

www.rsc.org/

Wei-Wei Zhou, Wang Zhao,* Feng-Wu Wang, Wen-Yan Fang, Dao-Fu Liu, Yi-Jun Wei, Mai Xu, Xing Zhao and Xian Liang

A rutile topological 3-D metal organic framework (MOF) had been obtained by reacting $\text{CdSO}_4 \cdot 8/3\text{H}_2\text{O}$ with HL (HL = 6-aminonicotinic acid) under solvothermal condition. Unique right- or left- handed helices can be found in the architecture of the MOF. The framework can exhibit tunable UV-to-visible fluorescence by variation of excitation light.

In recent years, tunable fluorescent materials attract more and more researcher's attention owing to their potential applications in sensing and lighting.¹ To our knowledge, the general approach to gain tunable fluorescence is to tailor the types and concentrations of activated ions.² Common examples include lanthanide or transition metal-doped materials,³ and lanthanide heterometallic complexes.⁴ Obviously, it is inconvenient and unsatisfying to control or handle emissions of these materials during use.

Metal-organic frameworks (MOFs) are coming into prominence as tunable luminescent materials,⁵ in which ligand-centered and metal-to-ligand charge transfer could coexist, making their fluorescence tunable by variation of excitation light.⁶ However, the preparation of tunable luminescent MOFs still faces challenges, since it is hard to control the tunability. In our opinion, the choice of ligands is very crucial. If the ligands themselves show tunable luminescence, their MOFs are most likely to produce tunable emissions, too.⁷ Especially when ligand-centered charge transition mixed with metal-to-ligand charge transfer (MLCT) or ligand-to-metal charge transfer (LMCT), further-enhanced variable tunable-luminescence can be exhibited to us. Ligand HL (HL = 6-aminonicotinic acid) is a good donor-accepter system with rich π electrons, and HL can exhibit UV-to-visible luminescence. We select the bridging ligand HL as sources to construct a novel Cd(II) compound $[\text{Cd}_3(\text{SO}_4)_2\text{L}_2(\text{H}_2\text{O})_4]_n$ (**1**). Herein, we report the synthesis, structure, topologic network, UV-to-visible luminescent properties, and band structure of **1**.

Compound **1** was prepared by solvothermal reaction‡ of

$\text{CdSO}_4 \cdot 8/3\text{H}_2\text{O}$ and HL at 170 °C for 4 days. The experimental and simulated powder X-ray diffraction (XRD) patterns are in good agreement with each other, suggesting the phase purity of the product (Fig. S1†). The structure of compound **1** was identified by satisfactory elemental analysis‡, IR (Fig. S2†) and single-crystal X-ray diffraction analysis§ (ESI†). The asymmetric unit of **1** contains one and half Zinc atoms, one L ligand, one sulfate group and four water molecules. The Cd2 atom is six-coordinated by one sulfate O14 atom, two water (O3W, O4W) oxygen atoms, and their symmetry-related atoms O14D, O3WD, O4WD ($D = -x, 1 - y, 1 - z$), yielding an almost octahedral environment, with the Cd2(II) center locating in the best least-squares plane of the four water-oxygen atoms (Fig. 1). However, the Cd1 atom has a distorted octahedral environment coordination, formed by two oxygen atoms (O1, O2) from two different L ligands, one N1 atom from another L ligand, one sulfate O11 atom and two water (O1W, O2W) oxygen atoms. The Cd–N distance is 2.317(3) Å and the Cd–O distances range from 2.222(3) to 2.453(3) Å. Thus, the sulfate anion links two Cd atoms (Cd1, Cd2) via its two oxygen atoms (O11, O14), acting as μ_2 -bridge. So we can see, two Cd1 atoms are connected to one Cd2 atom which is located at a crystallographic inversion center via two μ_2 -bridging sulfate groups, forming a zigzag trinuclear secondary building unit (SBU) (Fig. 2(a)). These bonding modes make the S1–O11–Cd1 angle 133.00(16)°, S1–O14–Cd2 angle 139.30(18)° and

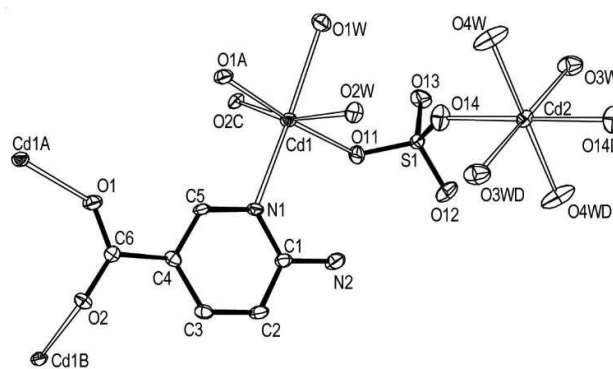


Fig. 1 ORTEP drawing of **1** with 50% thermal ellipsoids with hydrogen atoms being omitted for clarity. (Symmetry codes: A: $1 - x, 1 - y, 1 - z$; B: $1 - x, -1/2 + y, 3/2 - z$; C: $1 - x, 1/2 + y, 3/2 - z$; D: $-x, 1 - y, 1 - z$).

Anhui Key Laboratory of Low Temperature Co-fired Materials, College of Chemistry & Materials Engineering, Huainan Normal University, Huainan, Anhui 232038, People's Republic of China. E-mail: zwwz@live.com; Tel: +86 5546862556

† Electronic Supplementary Information (ESI) available: Figures showing structural details, TGA data, X-ray powder diffraction patterns, IR spectra, band structure, detailed PL spectrum of HL and **1**, diffuse reflection spectrum, tables for crystallographic data. See DOI: xxx

the intra-trinuclear Cd1...Cd2 separation 5.571(2) Å.

Each SBU connects to six neighboring L ligands in six directions via two Cd1-O1 bonds, two Cd1-O2 bonds and two Cd1-N1 bonds. Thus, this generates a six-connecting node in the structure of **1** (Fig. 2(a)). As for each L ligand, it shows a tridentate-coordinated mode with its O1, O2 and N1 atoms chelated to three Cd1 ions of three different SBUs, acting as a μ_3 -bridge. Thus, we can consider L ligands to be three-connecting nodes (Fig. 2(b)). As a result, the SBUs are interconnected through μ_3 -L ligands to generate a 3-D architecture (Fig. S4†). As mentioned above, the framework of **1** can be symbolized as a (3,6)-connected noninterpenetrating decorated rtl net [Schläfli symbol $(4\cdot6^2)_2(4^2\cdot6^{10}\cdot8^3)$] by considering L ligands and SBUs as 3- and 6-connected nodes (Fig. 2(c)).⁸ HL is a simple ligand, it can be easily obtained from commercial resources or synthesized in laboratories. However, metal-organic compounds containing HL or L⁻¹ ligands have not been reported till now. Compound **1** is an unprecedented coordination compound of 6-aminonicotinic acid ligand.

Moreover, we can find unique helices in the structure of **1**. The helix is constructed by carboxyl groups of L ligands (carboxyl A, seeing Fig. S5(a)†) bridging SBUs, displaying right-handed helical chains, with the pitch of the helix being 10.365 Å. The nearest Cd2...Cd2 distance is about 6.325 Å, and the shortest Cd1-Cd1 distance is 5.325 Å within a chain. All the helices are in an orderly arrangement along *b* direction. Adjacent helices link each other via the others carboxyl groups (carboxyl B, seeing Fig. S5(b)†) which have not participated in the formation of helices, extending the helical chains to generate a 2-D sheet structure (Fig. S5(b)†) in *bc*

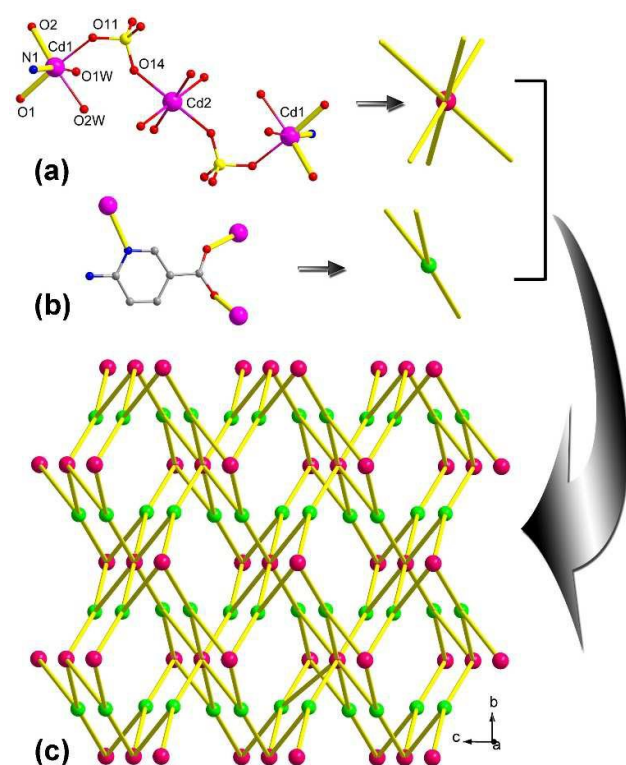


Fig. 2 (a) Simplified view of 6-connected zigzag trinuclear unit in **1**; (b) Simplified views of 3-connected L ligand in **1**; (c) A schematic view of the 3, 6-connected rtl net of 3-D supramolecular architecture of **1**.

plane. The nearest Cd2...Cd2 separation of the adjacent helical chains within a sheet is 7.251 Å. The adjacent layers are interlinked each other through interlamellar pyridine rings of L ligands to form the 3-D structure of **1** (Fig. 3(a), Fig. S5(c)†), with the nearest Cd2...Cd2 distances of the adjacent layers being 16.935 Å. Especially interesting, left-handed helices can be found if we choose carboxyl B groups to link SBUs (Fig. S6(a)†). The carboxyl A groups bridge the left-handed chains to form sheets in *bc* plane (Fig. S6(b)†). Furthermore, the parallel sheets are interlinked by pyridine rings, forming the 3-D structure of **1** (Fig. 3(b), Fig. S6(c)†). Carefully checking the reported decorated rtl nets,⁹ we have not found helices among them, except for the complex $[\text{ML}(\text{H}_2\text{O})_2]_n$ ($M = \text{Mn}, \text{Co}, \text{Zn}, \text{Cd}; \text{H}_2\text{L} = 5\text{-carboxyl-1-carboxymethyl-3-oxidopyridinium}$) reported by Feng and Jiang and co-workers.¹⁰ It is well known that inorganic anions may play a key role in the construction of the structures for complexes, because they can affect the coordination modes of the organic ligands.¹¹ In comparison with the known rtl-net complexes, the novel helices of **1** may be due to its zigzag trinuclear SBUs, which are related with the inorganic anions, sulfate anions. All these topological and structural properties enable **1** to

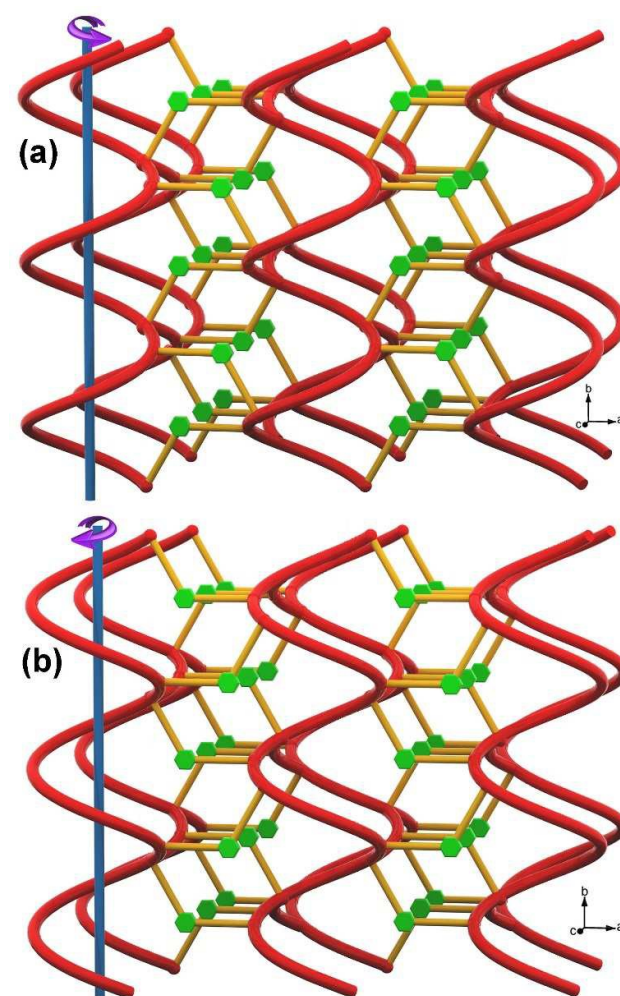


Fig. 3 Schematic presentation of the 3-D network of **1** containing (a) right-handed helical chains or (b) left-handed helical chains (green hexagons: pyridine rings).

be an excellent candidate for structural chemistry.

The diffuse reflection spectrum shows that **1** displays intense absorption bands in the UV (200–400 nm) range which reveals the presence of an optical gap of 3.50 eV, and some absorption in the infrared region (1400–2600) (Fig. S7 and S8[†]). The solid-state luminescence of **1** was investigated at room temperature. Three emission bands (A, B, C) can be found in the whole luminescence progress of **1** (Fig. 4, Fig. S9[†]). When excited at very wide range of 250–335 nm, compound **1** exhibits emission A with maxima at ~372 nm. It is notable that emission A has a very broad excitation band, and broad emission band in the range of 320–500 nm. Then as the excitation wavelength increases to the 340–365 nm band, the emission A becomes lower and a new emission maxima at ~387 nm (emission B) emerges. However, with the excitation light shifting to 370 nm or more, the intensity of emission B decrease rapidly, a maximum emission (emission C) centered at ~476 nm is observed. Notably, the bands of emission A, B and C are somewhat overlapping because of their broad bands and near emission peaks. In a word, the spectra of **1** is composed of three emission bands (emission A, B and C), while the intensities of the three bands show quite a different dependence on the excitation wavelength (Fig. S10[†]). When excited at shorter wavelength than 370 nm, emission A and B dominate the total emission spectrum. When excited at longer wavelength than 370 nm, emission C grows stronger accompanied by the decrease and disappearance of emission A and B. Consequently, compound **1** exhibits tunable UV-to-visible photoluminescence upon variation of excitation light. The free HL ligand displays three emissions (emission A', B' and C') and tunable UV-to-visible photoluminescence, too (Fig. S11 and S12[†]). Through the comparison between emissions spectra of **1** and HL, we can find that the emission A are similar to emission A' of ~367 nm peak, the peaks of emission B and C are with blue-shift of 41 nm and 52 nm compared to emission B' (centered at ~428 nm) and C' (centered at ~528 nm). Therefore, the three peaks of **1** can be tentatively ascribed to the fluorescence of the L ligand. The external quantum yield of **1** is 7% when excited by 350-nm light. The fluorescence decay curve of **1** excited by 350-nm light consists of fast and slow decay components. The decay curve can be well fitted by double exponential equation: $I(t) = I_0 + A \exp(-t/\tau_1) + B \exp(-t/\tau_2)$. The values of τ_1 and τ_2 extracted from the fitted curve are 1.02 and 4.08 ns, indicating that it has fluorescence characteristics (Fig. S14[†]).

The electronic structure of **1** was theoretically calculated in order to better understand its photoluminescent mechanisms (ESI[†]). On the grounds of theoretical-calculation results for **1**, the band structure shows an indirect band gap of 3.58 eV (Fig. S15[†]), which is comparable with the experimental value. The top of the valence bands (VBs) (from -3.5 to Fermi level (0 eV)) and the bottom of the conduction bands (CB) (from 3.0 to 4.5 eV) are dominated by p- π orbitals of L⁻¹ ligands (Fig. 5(a)). Accordingly, it can be considered that the observed spectral emissions of **1** can be mainly attributed to ligand-centered charge transitions based on L⁻¹ ligands. This results are in agreement with the above tentative ascription for the fluorescence of **1**. For deeper exploration, the density of states (DOS) of L⁻¹, py, NH₂, COO⁻¹, which are taken from the theoretical-calculation results for **1**, are detailed illustrated (Fig. 5(b)). For the total DOS of L⁻¹ ligand, the top of VBs

between energy -3.5 eV and Fermi level are mainly ascribed to the p- π orbitals of py group, p- π orbitals of COO⁻¹ group, mixed with p- π orbital of NH₂ group which mainly dominates -1.6 eV to -0.4 eV range. While the p- π^* antibonding orbitals of py

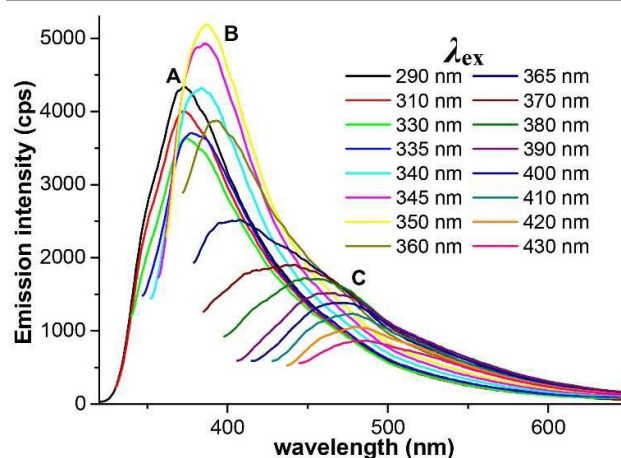


Fig. 4 Solid-state emission spectra of **1** by variation of the excitation light under the same conditions.

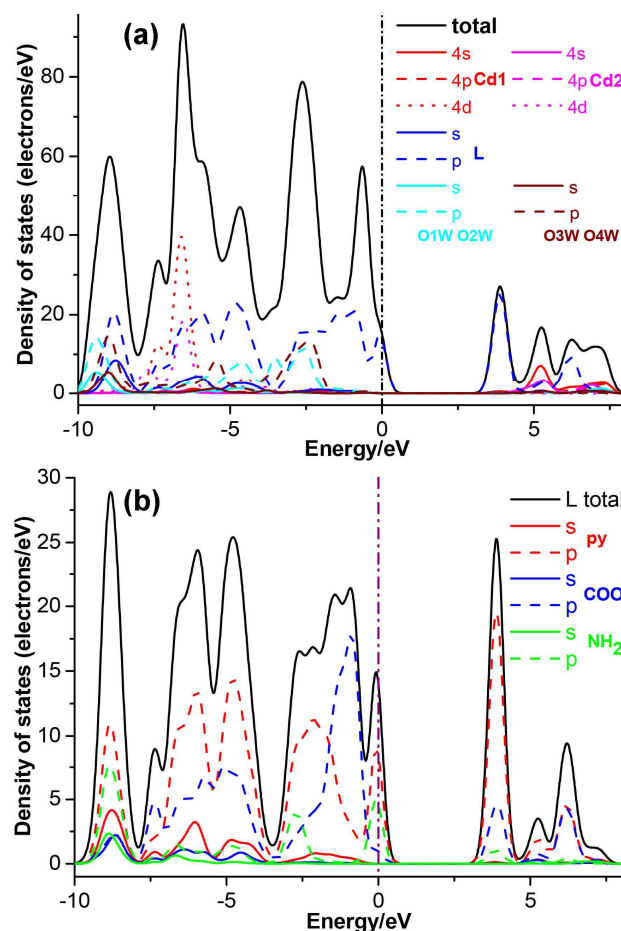


Fig. 5 (a) The total and partial DOS of **1**; (b) the total and partial DOS of L ligand which are taken from the theoretical-calculation results for **1**. The position of the Fermi level is set at 0 eV.

group mostly accounts for the CBs between energy 3.0 and 4.5 eV. Consequently, we can come into a conclusion that the emission A peak at ~372 nm mainly arises from intragroup π - π^* transition of py, similar emissions have been reported in the pyridine derivatives and pyridine-based complexes.¹² And emission C peak at 476 nm can be attributed to intergroup π - π^* transition from COO⁻¹ to py, Cai and co-workers have found this kind of emission.¹³ For emission B, it can be reasonably ascribed to π - π^* transition from NH₂ to py separately. We can also see the enhanced photoluminescence intensity of **1**, and the possible explanation is that the L⁻¹ ligand is deprotonated and coordinated to Cd(II) ions, which improves the rigidity of the ligand and reduces energy loss.¹⁴ Moreover, such a excitation broad bandwidth of **1** is qualified to improve the overlap with the excitation beam, hence making **1** adequate for applications. So we see that HL and its coordination compounds (CC) may exhibit tunable photoluminescence. And more variable emissions can be seen if MLCT occurs in the CCs, even white-light can be impossible.

Conclusions

In summary, we have prepared a 3-D unprecedented Cd(II) MOF based on 6-aminonicotinic acid. Compound **1** contains unique zigzag trinuclear SBUs, which is further bridged by L ligands, forming a (3,6)-connected noninterpenetrating rtl net. Moreover, novel right or left helical chains can be find in the structure of **1** via skillful selection of bridging carboxyl groups. Upon variation of excitation light, HL and **1** exhibit tunable UV-to-visible fluorescence, which make **1** a potential photoactive material in photophysical chemistry. More importantly, we find HL ligand is an excellent candidate for preparing tunable-fluorescent MOFs materials. This research may provide a new route to explore the fluorescent materials with tunable PL.

Acknowledgements

We gratefully acknowledge the financial support of the NSF of China (21201071, 61205213, 21176099), the NSF of Anhui Province (1208085QB42), and Science and Technology Project of Huainan City (2013A4105), and Program for Innovative Research Team in Huainan Normal University.

Notes and references

† Synthesis of **1**: A mixture of HL (55 mg, 0.4 mmol), CdSO₄·8/3H₂O (154 mg, 0.6 mmol), water (3 mL) and ethanol (6 mL) was loaded into a 25-mL Teflon-lined steel autoclave, and heated at 170 °C for 4 days, yielding colourless crystals of **1**. Yield: 60 % (based on Cd). Anal. calcd (%): C, 15.21; H, 2.77; N, 5.91. Found: C, 15.28; H, 2.74; N, 5.87.

§ Crystal data for **1**: C₁₂H₂₆Cd₃N₄O₂₀S₂, Mr = 947.69, Monoclinic, P2₁/c, a = 16.934(7), b = 10.365(4), c = 7.251(3) Å, β = 92.875(9)°, V = 1271.1(9) Å³, T = 293(2) K, Z = 2, ρ_{calcd} = 2.476 g/cm³, μ = 2.751 mm⁻¹. Final R indices [I > 2 σ (I)], R1 = 0.0376, wR2 = 0.0975. GoF on F² = 1.026. CCDC-1056408.

1 (a) A. Y.-Y. Tam, K. M.-C. Wong and V. W.-W. Yam, *J. Am. Chem. Soc.*, 2009, **131**, 6253; (b) S. Sapra, S. Mayilo, T. A. Klar, A. L. Rogach and J. Feldmann, *Adv. Mater.*, 2007, **19**, 569; (c) F. Wang, X. Xue and X. Liu, *Angew. Chem. Int. Ed.*,

2008, **47**, 906; (d) K. Jayaramulu, P. Kanoo, S. J. George and T. K. Maji, *Chem. Commun.*, 2010, **46**, 7906; (e) N. Pradhan, D. Goorskey, J. Thessing and X. Peng, *J. Am. Chem. Soc.*, 2005, **127**, 17586; (f) S. Zhou, N. Jiang, B. Zhu, H. Yang, S. Ye, G. Lakshminarayana, J. Hao and J. Qiu, *Adv. Funct. Mater.*, 2008, **18**, 1407.

2 (a) A. M. Kaczmarek and R. V. Deun, *Chem. Soc. Rev.*, 2013, **42**, 8835; (b) F. Auzel, *Chem. Rev.*, 2004, **104**, 139; (c) C. Feldmann, T. Jüstel, C. R. Ronda and P. J. Schmidt, *Adv. Funct. Mater.*, 2003, **13**, 511; (d) D. K. G. de Boer, D. J. Broer, M. G. Debije, W. Keur, A. Meijerink, C. R. Ronda and P. P. C. Verbunt, *Opt. Express*, 2012, **20**, A395.

3 (a) W. Zheng, P. Huang, D. Tu, E. Ma, H. Zhu and X. Chen, *Chem. Soc. Rev.*, 2015, **44**, 1379; (b) H. Xie, J. Lu, Y. Guan, Y. Huang, D. Wei and H. J. Seo, *Inorg. Chem.*, 2014, **53**, 827; (c) D. Tu, Y. Liu, H. Zhu, R. Li, L. Liu and X. Chen, *Angew. Chem. Int. Ed.*, 2013, **52**, 1128; (d) W. T. Fu, D. J. W. IJdo and A. Bontenbal, *J. Solid State Chem.*, 2013, **201**, 128; (e) L. R. Bradshaw, A. Hauser, E. J. McLaurin and D. R. Gamelin, *J. Phys. Chem. C*, 2012, **116**, 9300; (f) Y.-W. Li, S.-J. Liu, T.-L. Hu and X.-H. Bu, *Dalton Trans.*, 2014, **43**, 11470; (g) T.-L. Hu, R.-Q. Zou, J.-R. Li and X.-H. Bu, *Dalton Trans.*, 2008, 1302.

4 (a) L. Armelao, S. Quici, F. Barigelletti, G. Accorsi, G. Bottaro, M. Cavazzini and E. Tondello, *Coord. Chem. Rev.*, 2010, **254**, 487; (b) Z. Amghouz, S. García-Granda and J. R. García, *Inorg. Chem.*, 2012, **51**, 1703; (c) Y. Cui, B. Chen and G. Qian, *Coord. Chem. Rev.*, 2014, **273-274**, 76; (d) B. Chen, L. Wang, Y. Xiao, F. R. Fronczek, M. Xue, Y. Cui and G. Qian, *Angew. Chem. Int. Ed.*, 2009, **48**, 500; (e) K. Liu, H. You, Y. Zheng, G. Jia, Y. Song, Y. Huang, M. Yang, J. Jia, N. Guo and H. Zhang, *J. Mater. Chem.*, 2010, **20**, 3272.

5 (a) J. D. Furman, A. Y. Warner, S. J. Teat, A. A. Mikhailovskiy and A. K. Cheetham, *Chem. Mater.*, 2010, **22**, 2255; (b) J. B. Pollock, G. L. Schneider, T. R. Cook, A. S. Davies and P. J. Stang, *J. Am. Chem. Soc.*, 2013, **135**, 13676; (c) D. F. Sava Gallis, L. E. S. Rohwer, M. A. Rodriguez and T. M. Nenoff, *Chem. Mater.*, 2014, **26**, 2943; (d) T. Lasanta, M. E. Olmos, A. Laguna, J. M. López-de-Luzuriaga and P. Naumov, *J. Am. Chem. Soc.*, 2011, **133**, 16358.

6 (a) M.-S. Wang, S.-P. Guo, Y. Li, L.-Z. Cai, J.-P. Zou, G. Xu, W.-W. Zhou, F.-K. Zheng and G.-C. Guo, *J. Am. Chem. Soc.*, 2009, **131**, 13572; (b) L. Li, S. Zhang, L. Han, Z. Sun, J. Luo and M. Hong, *Cryst. Growth Des.*, 2013, **13**, 106.

7 S.-Q. Zhang, F.-L. Jiang, Y. Bu, M.-Y. Wu, J. Ma, X.-C. Shan, K.-C. Xiong and M.-C. Hong, *CrystEngComm*, 2012, **14**, 6394.

8 (a) Q.-Y. Liu, D.-Q. Yuan and L. Xu, *Cryst. Growth Des.*, 2007, **7**, 1832; (b) Z. Su, Z.-S. Bai, J. Fan, J. Xu and W.-Y. Sun, *Cryst. Growth Des.*, 2009, **9**, 5190; (c) G.-M. Sun, X.-F. Feng, H.-X. Huang, Z.-W. Liao, Y.-M. Song, X.-Z. Tian, S.-J. Liu and F. Luo, *Inorg. Chem. Commun.*, 2012, **16**, 43.

9 (a) Y.-C. He, J. Guo, H.-M. Zhang, J. Yang, Y.-Y. Liu and J.-F. Ma, *CrystEngComm*, 2014, **16**, 4210; (b) L. Xie, S. Liu, B. Gao, C. Zhang, C. Sun, D. Li and Z. Su, *Chem. Commun.*, 2005, 2402; (c) T. Liu, D. Luo, D. Xu, H. Zeng and Z. Lin, *Dalton Trans.*, 2013, **42**, 368; (d) J. Pan, F.-L. Jiang, D.-Q. Yuan, X.-C. Shan, M.-Y. Wu, K. Zhou, Y.-L. Gai, X.-J. Li and M.-C. Hong, *CrystEngComm*, 2013, **15**, 5673; (e) F. Luo, Y.-X. Che and J.-M. Zheng, *Eur. J. Inorg. Chem.*, 2007, 3906; (f) X. Zhao, G. Zhu, Q. Fang, Y. Wang, F. Sun and S. Qiu, *Cryst. Growth Des.*, 2009, **9**, 737.

10 M.-X. Jiang, C.-H. Zhan, Y.-L. Feng and Y.-Z. Lan, *Cryst. Growth Des.*, 2010, **10**, 92.

11 Q.-G. Zhai, C.-Z. Lu, X.-Y. Wu and S. R. Batten, *Cryst. Growth Des.*, 2007, **7**, 2332.

12 L. Li, J. Zhao, C. Wang, S. Yang and W. Hou, *Z. Anorg. Allg. Chem.*, 2012, **638**, 187.

13 L.-Z. Cai, M.-S. Wang, M.-J. Zhang, G.-E. Wang, G.-C. Guo and J.-S. Huang, *CrystEngComm*, 2012, **14**, 6196.

Journal Name

COMMUNICATION

- 14 (a) M. D. Allendorf, C. A. Bauer, R. K. Bhakta and R. J. T. Houk, *Chem. Soc. Rev.*, 2009, **38**, 1330; (b) Y. Cui, Y. Yue, G. Qian and B. Chen, *Chem. Rev.*, 2012, **112**, 1126; (c) V. J. Catalano and A. L. Moore, *Inorg. Chem.*, 2005, **44**, 6558.

RSC Advances Accepted Manuscript